

SUPERHRPD AND iMATERIA: SUPER HIGH RESOLUTION AND VERSATILE HIGH THROUGHPUT NEUTRON POWDER DIFFRACTOMETER AT J-PARC

Teguh Yulius Surya Panca Putra^{1,2}, Shuki Torii², Masao Yonemura², Ryoko Tomiyasu²,
Junrong Zhang², Miao Ping^{1,2}, Takashi Muroya², Setsuo Sato², Toru Ishigaki³, and
Takashi Kamiyama²

¹ The Graduate University for Advanced Studies (SOKENDAI),
SOKENDAI-KEK Office, 1-1 Oho, Tsukuba 305-0801, Japan

² High Energy Accelerator Research Organization, KEK Tokai Campus, Tokai 1-go kan,
203-1 Ohaza-Shirakata, Tokai-mura, Naka-gun, Ibaraki 319-1106, Japan

³ Ibaraki University, Hitachi, Ibaraki 316-8511, Japan

e-mail: panca@post.kek.jp

ABSTRACT

The Super High Resolution Powder Diffractometer (SuperHRPD) and the IBARAKI Materials Design Diffractometer (iMATERIA) at Materials and Life Science Facility (MLF), Japan Proton Accelerator Research Complex (J-PARC) are briefly described. Instrumental specification, including disk chopper system at both instruments is presented. Z-Rietveld, a Rietveld-refinement program for neutron powder diffraction data from both instruments has been developed. An example from CeO₂ analyses is given and the results show the reliability of instruments, data correction, and Z-Rietveld.

Keywords: SuperHRPD, iMATERIA, disk chopper, Z-Rietveld

INTRODUCTION.

There are variety of demands for neutron powder diffractometers such as suitable d -spacing resolution and range, high intensity on small samples, short time measurement, and reliable data analysis [1,2]. Motivated by these requirements, Super High Resolution Powder Diffractometer (SuperHRPD) and IBARAKI Materials Design Diffractometer (iMATERIA) were constructed at Materials and Life Science Facility (MLF), Japan Proton Accelerator Research Complex (J-PARC). SuperHRPD is characterized by its world best resolution $\Delta d/d = 0.03\%$ at $d < 4 \text{ \AA}$ and wide d -range $0.5 < d(\text{\AA}) < 60$ [3,4]. iMATERIA is a versatile neutron diffractometer with high throughput. It covers in d -range $0.18 < d(\text{\AA}) < 5$ with $\Delta d/d = 0.16\%$ at high resolution bank, and covers $5 < d(\text{\AA}) < 800$ with gradually changing resolution at three detector banks (90° , low angle and small angle)[2].

To access such d -spacing resolution and range, SuperHRPD and iMATERIA are equipped with a set of disk choppers, placed several meters from moderator. The use of multi-chopper allows the user to have a wide and continuous choice of wavelengths and d -range. A change in wavelength is achieved by changing the phase relationship between the disks.

A data analysis system was also prepared for the materials structural studies. Z-Rietveld is the software for the Rietveld analysis of powder diffraction data and implemented

in the Z-Code, a stand-alone software suit, distributed freely among users of time-of-flight (TOF) powder diffractometers that are installed at the MLF of J-PARC[5,6].

This paper will briefly describe SuperHRPD and iMATERIA including the disk chopper setting with example from neutron wavelength selection. Some results from neutron powder diffraction data collection with certain disk chopper setting and their data analysis using Z-Rietveld are also presented.

SuperHRPD and iMATERIA.

General specifications.

SuperHRPD is a neutron powder diffractometer at Beam Line 08 (BL-08), MLF, J-PARC. This diffractometer is designed to look at a decoupled poisoned hydrogen moderator and to have 31.2 m curved guide and 51.4 m straight guide length. The primary flight path (L_1) approximately 94.2 m and secondary flight path (L_2) about 2.5 m giving total flight path of approximately 94.7 m. iMATERIA is a high-efficiency, general-purpose neutron diffractometer for the analysis of crystal structure of powder samples over a wide d -range (Q -range). It looks at a decoupled poisoned hydrogen moderator (thicker side) and it has incident flight path (L_1) of 26.5 m, with straight neutron guides of 14.0 m. The layout of BL-08 and BL-20, where SuperHRPD and iMATERIA situated, is depicted in Figure 1 and the instrumental parameters [2,3] are overviewed in Table 1.

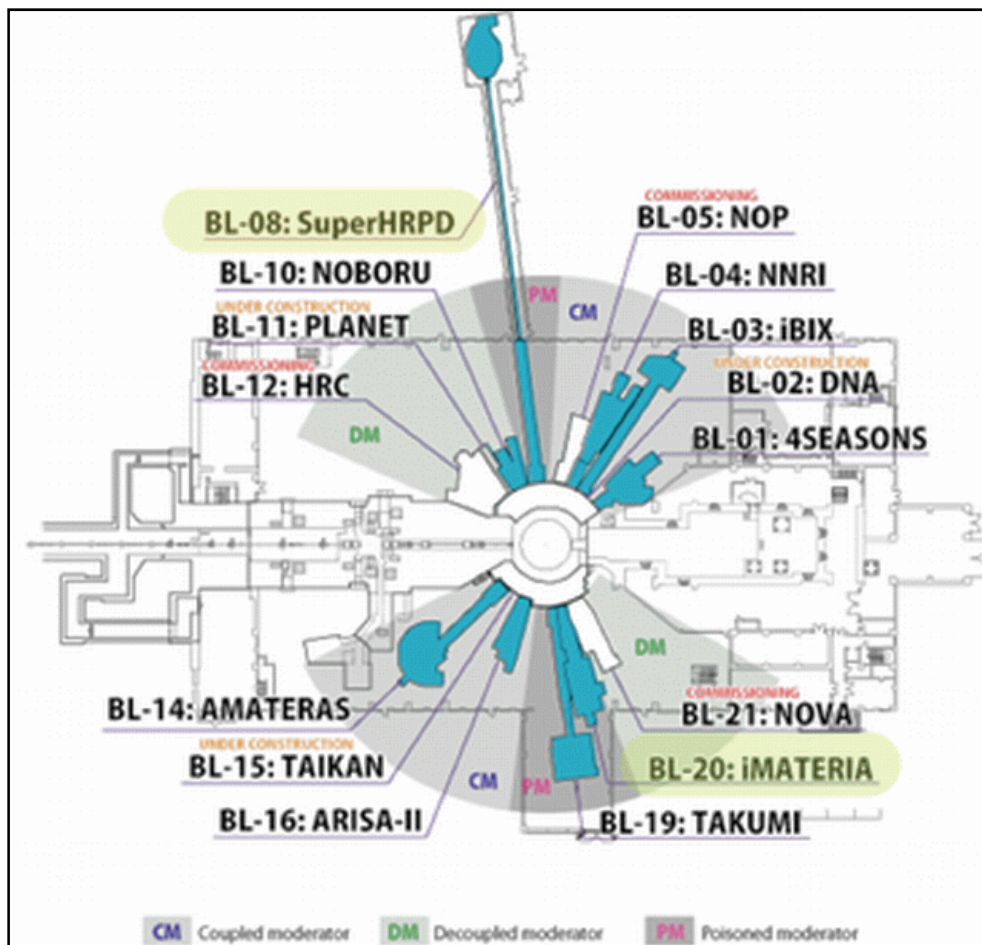


Figure 1: Layout of beamlines at J-PARC showing the location of SuperHRPD(BL-08) and iMATERIA (BL-20) at MLF, J-PARC.

Table 1: Instrumental parameters of SuperHRPD and iMATERIA.

SuperHRPD (Beam line 08)		iMATERIA (Beam line 20)	
Moderator: poisoned decoupled hydrogen moderator			
Position for disk choppers (wavelength-selection choppers)			
7.1m (single)		7.5m (double)	
12.725m &		11.25m (single)	
12.775m (both as double)		18.75m (single)	
Best resolution	0.03% @ $2\theta \approx 172^\circ$	High-resolution bank	
		Range of d -spacing	$0.09 \leq d(\text{\AA}) \leq 5.0$
		Resolution $\Delta d/d$	$\sim 0.16\%$
		2θ	$150^\circ \leq 2\theta \leq 175^\circ$
		L_2	2.0 – 2.3 m
Backscattering bank		Special environment bank	
Range of d -spacing	0.3 – 4.0 \AA	Range of d -spacing	$0.127 \leq d(\text{\AA}) \leq 7.2$
Resolution $\Delta d/d$	0.1 – 0.15 %	Resolution $\Delta d/d$	$\sim 0.5\%$
2θ	$150^\circ \leq 2\theta \leq 175^\circ$	2θ	$80^\circ \leq 2\theta \leq 100^\circ$
L_2	2 m	L_2	1.5 m
90° bank		Low angle bank	
Range of d -spacing	0.4 – 7.5 \AA	Range of d -spacing	$0.37 \leq d(\text{\AA}) \leq 58$
Resolution $\Delta d/d$	0.4 – 0.7 %	Resolution $\Delta d/d$	$\sim 1.9\% @ 40^\circ$
2θ	$60^\circ \leq 2\theta \leq 120^\circ$	2θ	$10^\circ \leq 2\theta \leq 40^\circ$
L_2	2 m	L_2	1.2 – 4.5 m
30° bank		Small angle bank	
Range of d -spacing	0.6 – 45 \AA	Range of d -spacing	$1.69 \leq d(\text{\AA}) \leq 800$
Resolution $\Delta d/d$	0.7 – 3.0 %	Resolution $\Delta d/d$	$\sim 5\%$
2θ	$10^\circ \leq 2\theta \leq 40^\circ$	2θ	$0.7^\circ \leq 2\theta \leq 5^\circ$
L_2	2.39 m	L_2	4.5 m

Figure 2 illustrates an overall schematic plan view of SuperHRPD and iMATERIA at MLF, J-PARC. Beam shutter and Fe-collimator are installed immediately after the moderator (not shown in the figure). This figure shows the position of the disk choppers at both instruments. Three wavelength-selection disk choppers were installed both in SuperHRPD and iMATERIA. Curved neutron guide with the length of 31.2 m was installed in SuperHRPD to block fast neutron from the prompt pulse coming from the moderator. For this purpose, T_0 -chopper will be installed in iMATERIA at position of 10.53 m. Straight neutron guide is used to conduct and to enhance the intensity of short wavelength neutrons to the sample area.

The disk choppers.

1. Description of the disk choppers.

SuperHRPD and iMATERIA employ multi-chopper system to select wavelength for neutron experiment. Two advantages will be achieved by using this system; the maximum speed of the disk chopper system is doubled by using counter rotating multi-chopper system, and any undesired wavelength from delayed neutron, for example slower neutrons from overtaken by faster neutrons from the succeeding pulse, will be blocked. Figure 3 (a), (b) and

(c) exemplifies the disk choppers as used in SuperHRPD, and Figure 3 (d) shows perspective of neutron beam guide and the disk chopper.

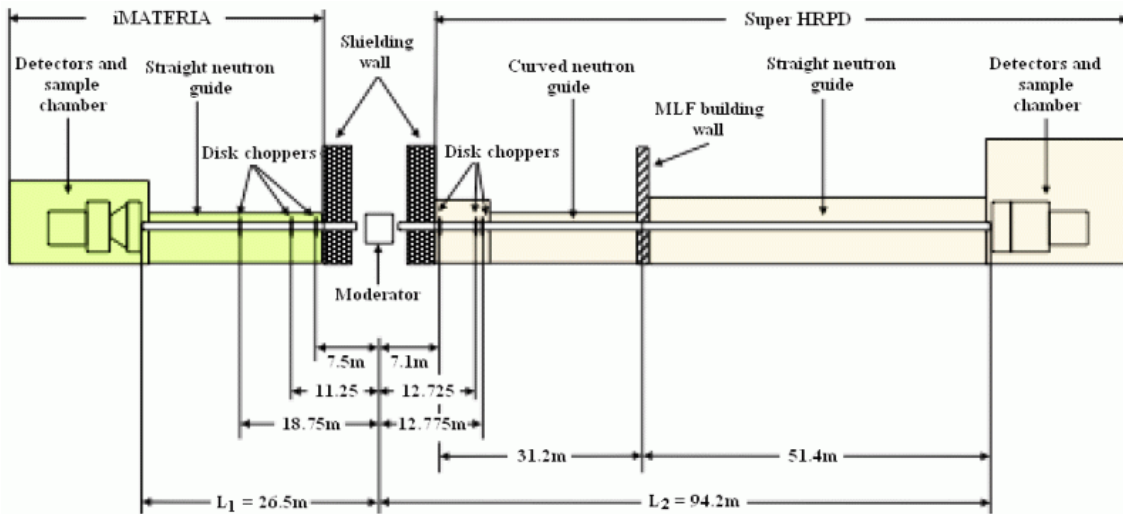


Figure 2: A conceptual figure showing the position of disk choppers currently used in SuperHRPD and iMATERIA.

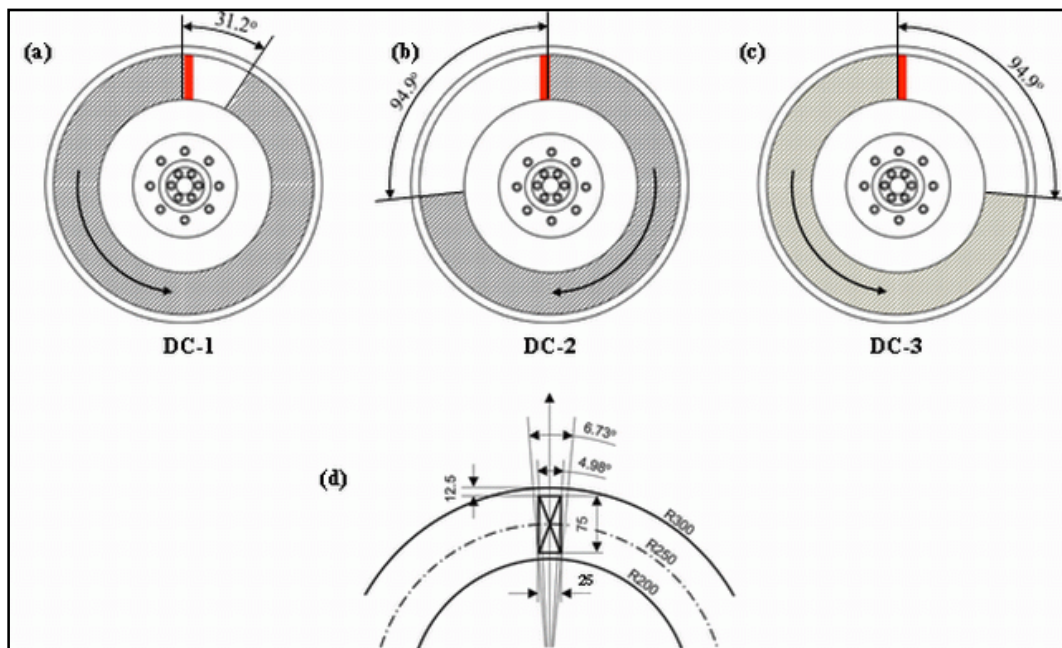


Figure 3: (a) disk chopper-1 (single), (b) disk chopper-2 and (c) disk chopper-3 (both as double) currently used in SuperHRPD. All disk choppers show the position of phasing 0° and the leading edge of each disk chopper where rotation will be started, relative to the position of the beam guide (shown in red rectangles). The arrows show typical direction of the rotation. (d) the perspective of neutron beam guide and the disk chopper. (dimensions are in mm).

The importance of the operation of multi-chopper system is represented in the path-time diagram shown in Figure 4. Disk chopper-1 (DC1) acts as a single disk and is used to select a wavelength band (inclined solid lines in Fig. 4), while both DC2 and DC3 act as double disks and are used to block any delayed neutrons from different time frame (dashed lines in Figure 4).

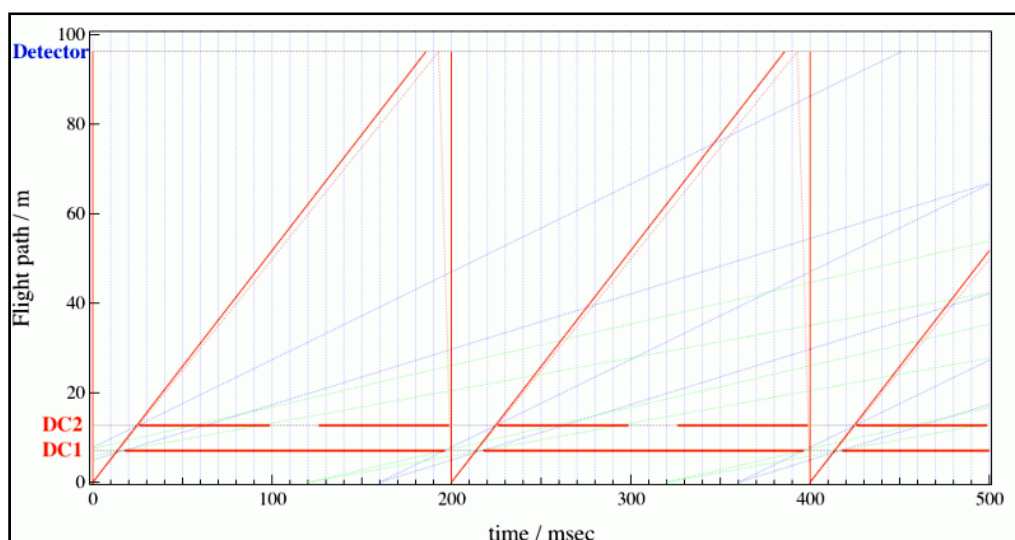


Figure 4: Path-time diagram of the time-of-flight diffractometer SuperHRPD. The rotation speed of DC1 (single) and DC2 (double) is 5 Hz and 10 Hz, respectively. The DC1 select wavelength band, whereas DC2 block delayed neutrons from different time frame (blue and green dashed lines). The inclined solid lines show the wavelength band from 0.006 to 7.650 Å.

Table 2: Specification of disk choppers at SuperHRPD and iMATERIA.

<i>SuperHRPD</i>		<i>iMATERIA</i>	
Single disk chopper (DC1)		Double disk chopper (DC1)	
Distance	7.1 m	Distance	7.5 m
Radius	0.3 m	Radius	0.35 m
Slit opening angle	31.2°	Slit opening angle	177°
Rotational speed	at some multiple or sub-multiple of 25 Hz (the source frequency)	Rotational speed	25 Hz
Double disk chopper (DC2)		1st Single disk chopper (DC2)	
Distance	12.725 m & 12.775 m	Distance	11.25 m
Radius	0.3 m	Radius	0.35 m
Slit opening angle	94.9°	Slit opening angle	134°
Rotational speed	at some multiple or sub-multiple of 25 Hz (the source frequency)	Rotational speed	12.5 or 25 Hz
<i>Note:</i>		2nd Single disk chopper (DC3)	
-	Rotational speed of the disk choppers is a combination of selected speed, for example DC1/DC2/DC3 = 5 Hz/10 Hz/10 Hz etc.	Distance	18.75 m
-	Typical direction of rotation is: DC1/DC2/DC3 = clockwise/counter-clockwise/clockwise	Radius	0.35 m
		Slit opening angle	217°
		Rotational speed	12.5 or 25 Hz
Wavelength-width (example)			
	7.602 Å		9.871 Å
Slit opening angle of DC1/DC2	31.2°/94.9°	Slit opening angle of DC1/DC2/DC3	176.5°/133.3°/217.4°
Rotational speed of DC1/DC2	5 Hz/10 Hz	Rotational speed of DC1/DC2/DC3	25 Hz/12.5 Hz/12.5 Hz

Table 2 enlisted the specification of the disk chopper used in SuperHRPD and iMATERIA. The rotation speed of the disk choppers is at some multiple or sub-multiple of the source frequency and is kept very precisely in phase with the source. Different mode of selection for disk choppers speed is possible for different analysis. For instance, at iMATERIA in normal mode for most of the application, the rotation speeds for the three disk choppers are selected to be the same with the pulse repetition rate 25 Hz. It will cover $0.18 < d(\text{\AA}) < 2.5$ with $\Delta d/d = 0.16\%$, and cover $2.5 < d(\text{\AA}) < 400$ with gradually changing resolution. At the speed of 12.5 Hz (wide- d mode), it is accessible to a wider d -range, $0.18 < d(\text{\AA}) < 5.0$ with $\Delta d/d = 0.16\%$, and $5.0 < d(\text{\AA}) < 800$ with gradually changing resolution.

2. Neutron wavelength selection by disk chopper phasing

An example of typical configuration of the disk choppers and neutron guide as used in SuperHRPD is shown in Figure 5. A single disk (DC1) is used to select wavelength of the neutrons from prompt pulse coming from the moderator. A counter rotating pair of disk choppers (DC2 and DC3) is working as a double disk to block the undesired wavelengths.

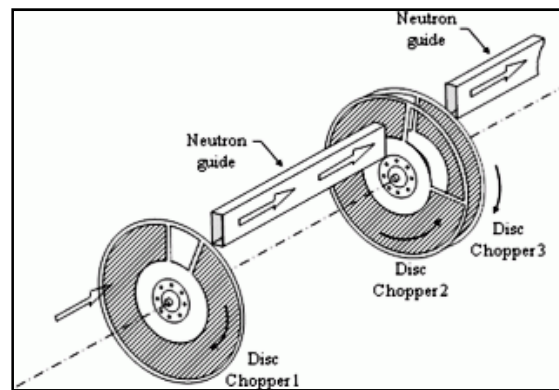


Figure 5: A schematic view of primary section showing the set up of disk choppers currently used in SuperHRPD. Moderator, beam shutter, Fe-collimator and sample area are not shown. The distances in the figure are not to scale the actual set up.

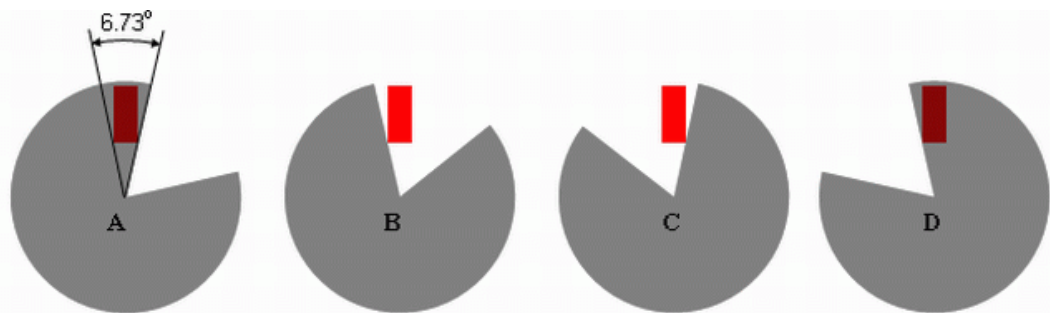


Figure 6: The sequence of event during the chopping of neutron beam by a disk chopper. In order to understand this basic sequence, the reader is asked to imagine that the window of the disk is about to open at the same time when the pulsed neutron beam come as shown in *a*; the neutron guide is represented by the red rectangle and the disk choppers are shown in transparency for clarity. Wavelength-width is selected through the sequence from A until D.

During rotation, a disk chopper will follow the sequence as shown in Figure 6. This figure is shown with the assumption that the disk chopper starts to open at the time of pulsed neutron beam reach it. Some expressions can be derived from this instance, regardless the starting point of the disk chopper to rotate. The time and wavelength when the leading edge

of the disk chopper is about to open until it is fully opened to the pulsed neutron beam with angular size of 6.73° (A to B in Figure 6) are given by:

$$t_{\theta_1}(\text{m sec}) = \frac{6.73^\circ}{2\pi f(\text{Hz})} \times 1000 \quad (2.1)$$

$$\lambda_1(\text{\AA}) = 3.956 \frac{t_{\theta_1}(\text{m sec})}{L(\text{m})} \quad (2.2)$$

where f is the frequency of the disk chopper L is the distance of the disk chopper from moderator. The time and wavelength when a disk chopper is fully open to the pulsed neutron beam (B to C in Figure 6) are given by:

$$t_{FDC1}(\text{m sec}) = \frac{\theta_F(\text{deg.})}{2\pi f(\text{Hz})} \times 1000 \quad (2.3)$$

$$\lambda_2(\text{\AA}) = 3.956 \frac{t_{FDC1}(\text{m sec})}{L(\text{m})} \quad (2.4)$$

where θ_F is the distance covered by the rotation of the disk chopper during this time. Finally, the time and wavelength when the closing edge of the disk chopper is about to close until it fully closed to the pulsed neutron beam (C to D in Figure 6), again are given by Eq. (2.1) and (2.2).

A change in desired wavelength is accessible by changing the phase of a disk or phase relationship between the disks. In this situation, the assumption taken as a basis for explanation as shown in the Figure 6 is modified. There will be a time shift for the disk to be opened. Pulsed neutrons beam might come before or after the disk is opened. An example as shown in Figure 7 is presented to explain a phasing for a disk chopper. Figure 7(a) shows the direction of rotation of the disk chopper as shown by the blue arrow, while a positive phasing is achieved by a counter-clockwise rotation (red arrow), and negative phasing by clockwise rotation (green arrow). The magnitude of the phasing is determined from the position of 0° phasing as shown in Figure 7(a), and the new starting points to rotate after $+10^\circ$ and -10° phasing are shown in Figure 7(b) and 7(c), respectively.

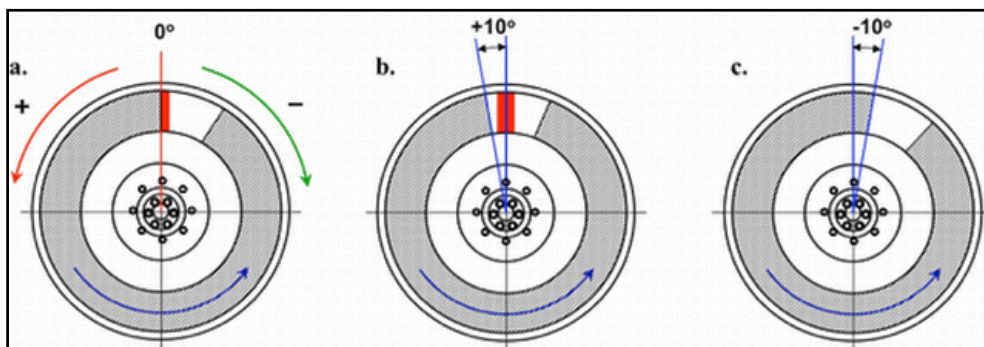


Figure 7: The disk chopper shown at the position of (a) 0° , (b) $+10^\circ$ and (c) -10° phasing. The blue arrow shows the direction of rotation of the disk chopper as neutrons (red rectangle) come from behind the disk chopper. The red and green arrows show positive and negative phasing, respectively.

The neutron is pulsed from the source in a certain frequency and each pulse or bunch consists of a band of wavelengths and they travel and spread out in time along [7] the beam guide before being ‘chopped’ by the disk chopper and pass through its window. The rotation

speed of the disk choppers is set at some multiple or sub-multiple of the source frequency and is kept very precisely in phase with the source. By applying a different phasing, a disk chopper would chop a different area of the bunch, i.e. wavelength, because different phasing will:

1. create different starting point for the disk to rotate relative to the time when the pulsed neutron beam come,
2. determine how long the window will be opened to these pulsed neutron beam, and, therefore
3. select different part of the pulsed neutron beam consists of certain wavelengths.

A new starting point as in (1) will cause a shift in time between the pulsed neutrons beam and the opening of the disk chopper. Positive phasing will select an area differs from the negative phasing, and each phasing will also determine the opening duration in related area.

In the case of positive phasing, as exemplify in Figure 8, it is easy to understand that the greater the phasing, the shorter the distance (θ_A) for the disk to rotate until it fully closed (from A to B in Figure 8). It means that the opening duration is shorter as well, thus resulting in shorter wavelength-width. Note that the pulsed neutron beam comes to the disk immediately after the disk is opened. The ‘early part’ (faster neutron) of the bunch will pass through the window, and the ‘later part’ (slower neutron) will be blocked by the disk. At some points, positive phasing will select low intensity neutrons and when the disk phasing is not synchronous with the pulsed neutron anymore, all neutrons will be blocked by the disk.

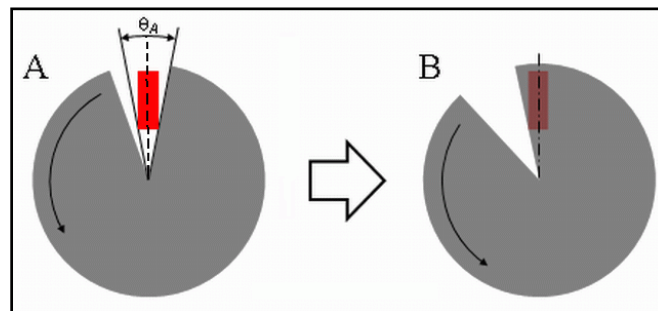


Figure 8: A representation of a disk chopper in *positive* phasing. Note that the pulsed neutron beam comes after the disk is opened. The opening time of the disk, represented by the distance of rotation (θ_A) to be fully closed to the pulsed neutron beam (from A to B), and the rotation direction are indicated. The neutron guide is represented by the red rectangle and the disk choppers are shown in transparency for clarity.

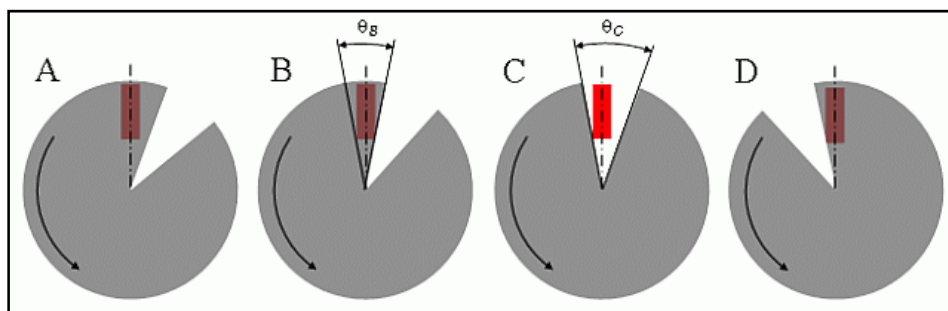


Figure 9: A representation of a disk chopper in *negative* phasing. Note that the pulsed neutron beam comes when the disk is still closed. The opening time of the disk is shown from B to C and is represented by rotation distance ($\theta_B + \theta_C$). The rotation direction is indicated and the neutron guide is represented by the red rectangle and the disk choppers are shown in transparency for clarity.

In the case of negative-phasing, as described in Figure 9., it should be emphasized that the pulsed neutron beam comes to the disk when it is still closed (example in A of Figure 9); therefore, the selected wavelength-width is the ‘later part’ (slower neutron) of the neutron bunch. The calculation for opening duration is based on the stage when the window starts to open until it fully closed (from B until D in Figure 9) and the distance is the combination of θ_B and θ_C . Greater negative-phasing will increase θ_B , or in other word, it will increase delay time for the disk to be opened to the pulsed neutron beam. The value of θ_C remains constant regardless of how large the negative phasing change, which means that wavelength-width remains constant as well. As negative phasing getting larger, selected wavelength-width will approach towards the tail of the neutron spectrum from the moderator. This part of neutron spectrum has low intensity; the disk will block all of the neutrons when the negative phasing is too large.

An example of wavelength selection by disk chopper is described in Figure 10. The figure shows which part of neutron spectrum selected by the disk chopper with $+20^\circ$ and -20° phasing, from the entire spectrums of the pulsed neutron from moderator. Comparing these spectrums, we see that positive phasing selected an area at the early parts of the spectrum of pulsed neutron from the moderator, while negative phasing selected the tail area. Selected wavelength-width tends to be narrower as positive phasing increases, while increasing negative phasing does not change selected wavelength-width.

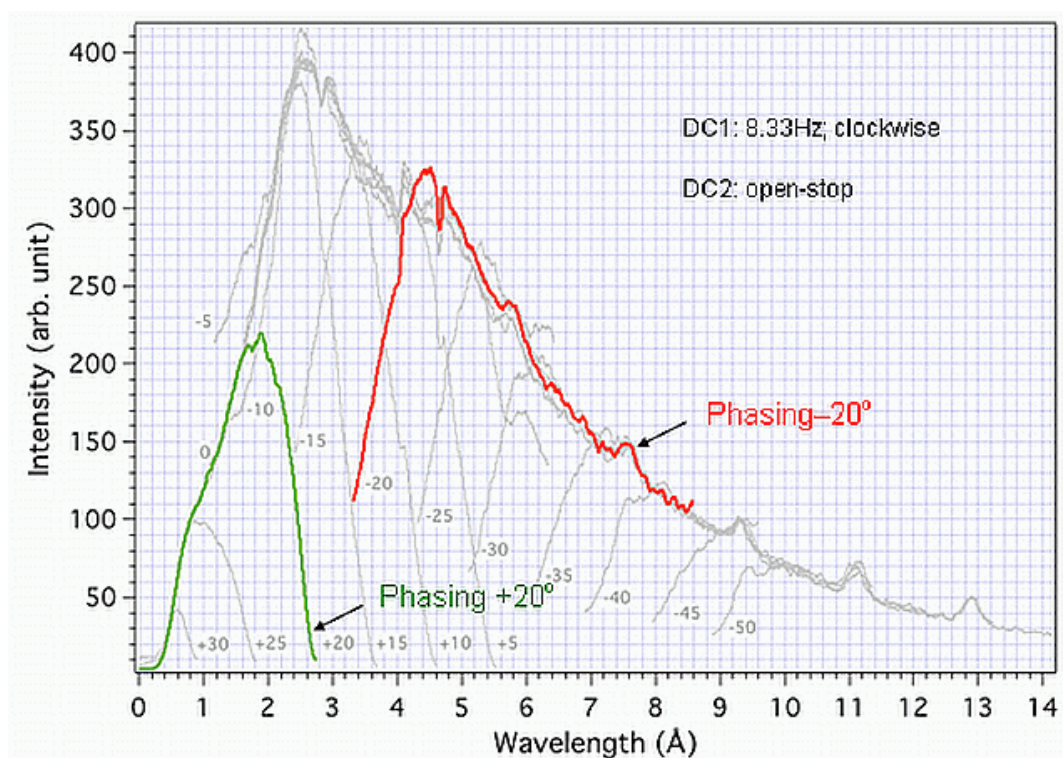


Figure 10: Pulsed neutron spectrums from monitor counter taken with various phasing. The selected areas by -20° and $+20^\circ$ phasing are presented in color. The spectrums shown in gray are the part of all neutron spectrums from moderator of the pulsed source.

A more thorough picture is represented in Figure 11, showing neutron spectrums from monitor counter, placed approximately 90 meters from the source; the phases of the wavelength-selection disk chopper (DC1) were varied from -50° until $+30^\circ$ in 5° increment. These spectrums are seen to change consistently with various phasing, with pronounced shift of the selected wavelength-width. Each phasing of DC1 picked out an area of wavelength-

width from initial neutron beam leaving the moderator and gave different neutron spectrums. The result is summarized in Table 3. The DC1 chopped the neutron beam into burst and these neutrons spread out in time and were in a well-defined burst.

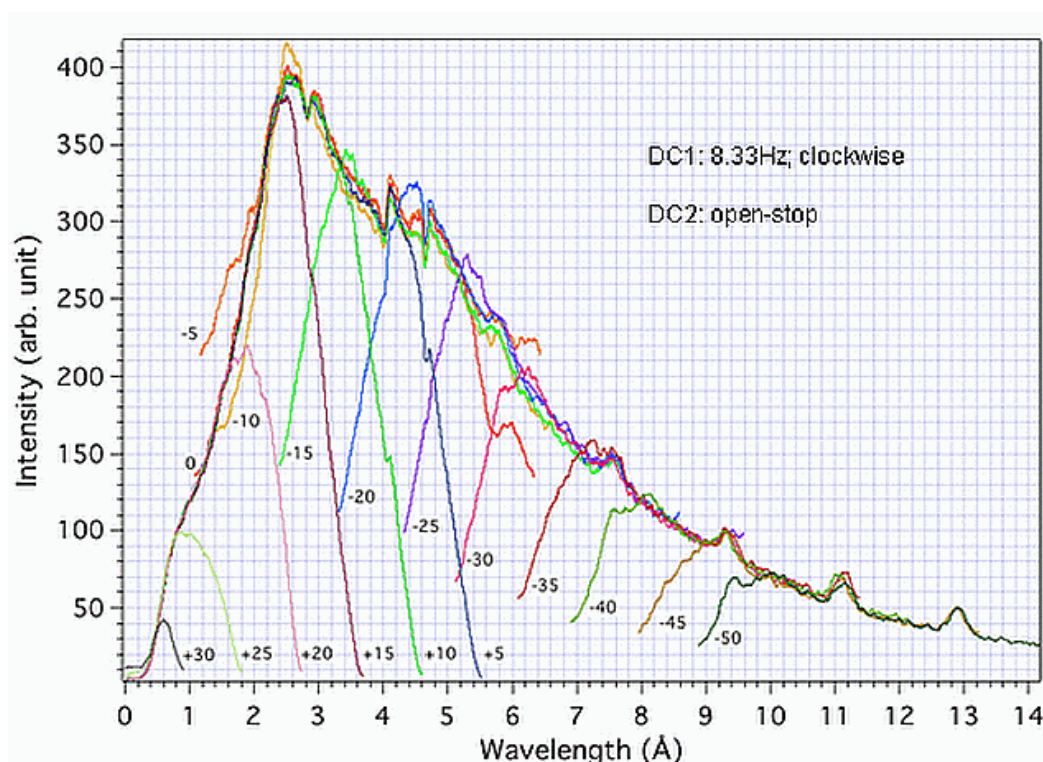


Figure 11: Pulsed neutron spectrums from monitor counter resulted in various DC1 phasing showed in corresponding values.

Table 3: Wavelengths and wavelength-width for various phasing of disk chopper 1 (DC1) at SuperHRPD. The rotation speed of DC1 is 8.33 Hz, while DC2 and DC3 were open stopped

Phasing (°)	$\lambda_1(\text{Å})$	$\lambda_2(\text{Å})$	$\lambda_{\text{width}}(\text{Å})$
30	0	0.91	0.91
25	0	1.81	1.81
20	0	2.74	2.74
15	0	3.70	3.70
10	0	4.60	4.60
5	0.25	5.52	5.27
0	1.07	6.34	5.27
-5	1.16	6.43	5.27
-10	1.37	6.64	5.27
-15	2.40	7.67	5.27
-20	3.31	8.58	5.27
-25	4.32	9.59	5.27
-30	5.12	10.39	5.27
-35	6.10	11.37	5.27
-40	6.90	12.17	5.27
-45	7.96	13.23	5.27
-50	8.89	14.16	5.27

The detectors.

Figure 12 illustrates the layout of three detector banks in SuperHRPD; backscattering bank, 90° bank and 30° bank. Fig. 10 depicts the layout of four detector banks in iMATERIA including a low angle and a small angle scattering detector banks. The important parameters of the detectors in both instruments are listed in Table 1. These detector banks were installed to accommodate the requirements or criteria in a versatile time of flight (TOF) diffractometer. Each detector bank comprised of one-dimensional ³He position-sensitive detectors (1D-PSDs). Each PSD has a diameter of 1.27 cm and an effective length of 60 cm [1]. Recently, the detector banks in SuperHRPD accommodate 704 PSDs from totally 1504 PSDs possibly installed.

The purpose of the design of iMATERIA does not require super high resolution. It is planned to be a high throughput diffractometer, and for this purpose intermediate resolution around $\Delta d/d = 0.15\%$, matched with high intensity and wide d coverage, is more necessary [2].

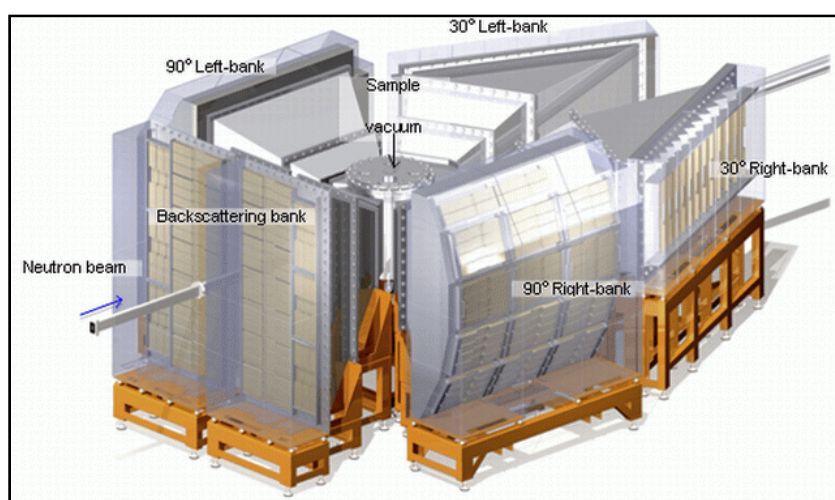


Figure 12: An illustration of the SuperHRPD instrument showing the layout of PSDs surround a vacuum chamber in which neutrons hit and are diffracted by a sample.

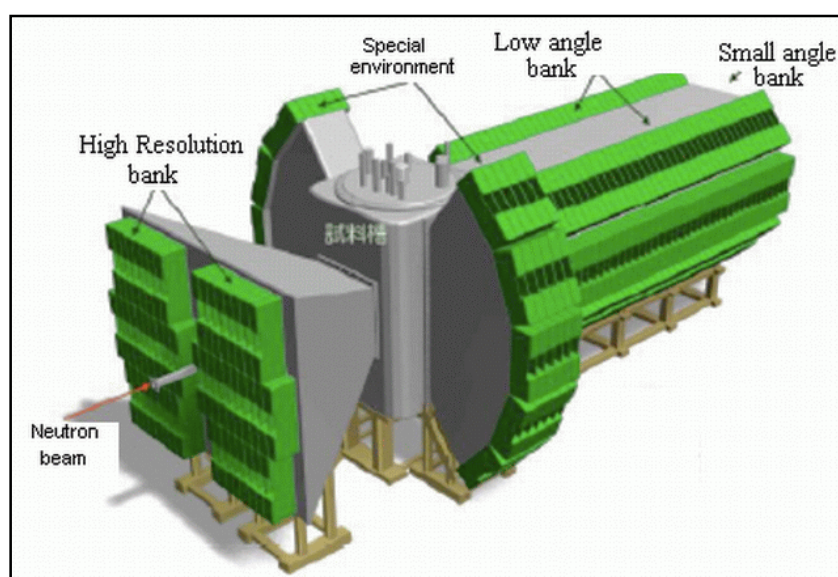


Figure 13: An illustration of the iMATERIA instrument showing the layout of detector banks.

The detector arrangement for each bank of SuperHRPD, as shown in Figure 13, shows separation into right and left sub-banks. This kind of arrangement will increase counting rate in powder diffraction experiment and also the data collection efficiency. The backscattering bank comprises two sub-bank arranged vertically. Recent measurement of diamond sample shows the resolution for Bragg reflection of (220) and (311) peaks are $\Delta d/d = 0.093\%$ and 0.089% , respectively. The 90° bank also comprises two sub-banks. The same measurement resulted in resolution $\Delta d/d = 0.42\%$ and 0.41% , respectively. The 30° banks comprises two sub-bank as well and the measurement resulted in resolution $\Delta d/d = 0.79\%$ and 0.75% , respectively.

Example of powder diffraction data measurement at SuperHRPD and iMATERIA.

In this section, a comparison of the results from powder diffraction measurement between SuperHRPD and iMATERIA taken under different setting of disk chopper is described. Figure 14 shows the result from powder data measurement of CeO_2 taken from both instruments. The powder diffraction data from SuperHRPD were collected with disk chopper speed of 5 Hz giving d -range up to 4.12 \AA , while the disk chopper speed of 12.5 Hz in iMATERIA resulted in d -range up to 5.63 \AA . With each setting, both instruments could identify all Bragg peaks from CeO_2 within their d -range.

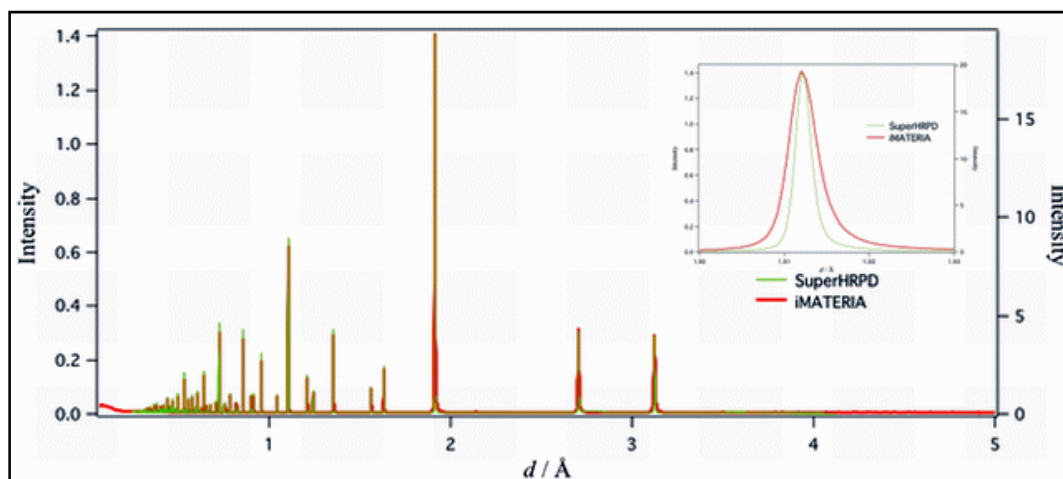


Figure 14: Neutron powder diffraction pattern of CeO_2 taken from SuperHRPD and iMATERIA. The difference in the peak shape between the diffraction patterns taken from SuperHRPD and iMATERIA as shown in the inset is due to the difference in instrumental resolution, where SuperHRPD have better resolution due to its longer flight path (see Figure 2).

Rietveld analysis of powder diffraction data by using Z-Rietveld.

Z-Rietveld can analyze X-ray, angle dispersive and time-of-flight (TOF) neutron diffraction data. It is also possible to execute multi-phase analyses and multi-histogram analyses including simultaneous analyses of X-ray and neutron data. The functions in Z-Rietveld will help untrained users of high throughput diffractometers such as iMATERIA to carry out reliable powder diffraction data analyses. An example of the powder diffraction data analysis of CeO_2 is presented. It was carried out with the help of Z-Rietveld, which is implemented in the Z-Code. The consideration for CeO_2 taken is as follow: cubic crystal structure, space group $Fm-3m(225_1)$, and $a = 5.411651 \text{ \AA}$.

1. Crystal structure refinement

The mathematical procedures implemented in Z-Rietveld has been reported [5,6] and explained in detail elsewhere [8]. The weighed residual factor R_{wp}^2 (' R -weighted pattern')

is the most meaningful of R 's because the numerator is the residual being minimized. For the same reason, it is also the one that best reflects the progress of the refinement and is defined as

$$R_{wp}^2 = \frac{\sum_i w_i (y_i^{obs} - y_i^{cal})^2}{\sum_i w_i (y_i^{obs})^2} \quad (3.1)$$

where y_i^{obs} and y_i^{cal} are the observed and calculated data points, and w_i is weighting factors taking into account the statistical accuracy of the diffraction experiment. The residual factor or 'R-pattern' itself is defined as

$$R_F = \frac{\sum_i |y_i^{obs} - y_i^{cal}|}{\sum_i y_i^{obs}} \quad (3.2)$$

The 'goodness-of-fit' indicator, S^2 , was also used and is defined as

$$S^2 = \frac{R_{wp}^2}{R_e^2} = \frac{\sum_i w_i (y_i^{obs} - y_i^{cal})^2}{N - P} \quad (3.3)$$

where N is the number of experimental observations, P is the number of refined parameters, and R_e^2 or 'R-expected' is defined as

$$R_e^2 = \frac{N - P}{\sum_i w_i (y_i^{obs})^2} \quad (3.4)$$

Another commonly used R -values are R_B ('R-Bragg') and R_F ('R-structure factor') as followed

$$R_B = \frac{\sum_f |I_f^{obs} - I_f^{cal}|}{\sum_f I_f^{obs}} \quad (3.5)$$

$$R_F = \frac{\sum_j |F_j^{obs}| - |F_j^{cal}|}{\sum_j |F_j^{obs}|} \quad (3.6)$$

where I_j is the intensity assigned to the j th Bragg reflection at the end of the refinement cycles and F_j^{obs} is

$$|F_j^{obs}|^2 = \frac{I_j^{obs}}{I_j^{cal}} \times |F_j^{cal}|^2 \quad (3.7)$$

In the expressions for R_B and R_F the "obs" (for observed) is put in quotation marks because the Bragg intensity, I_j , is rarely observed directly; instead the I_j values are obtained from programmatic allocation of the total observed intensity in a 'scramble' of overlapped reflections to the individual reflections according to the ratios of those reflection intensities in the calculated pattern.

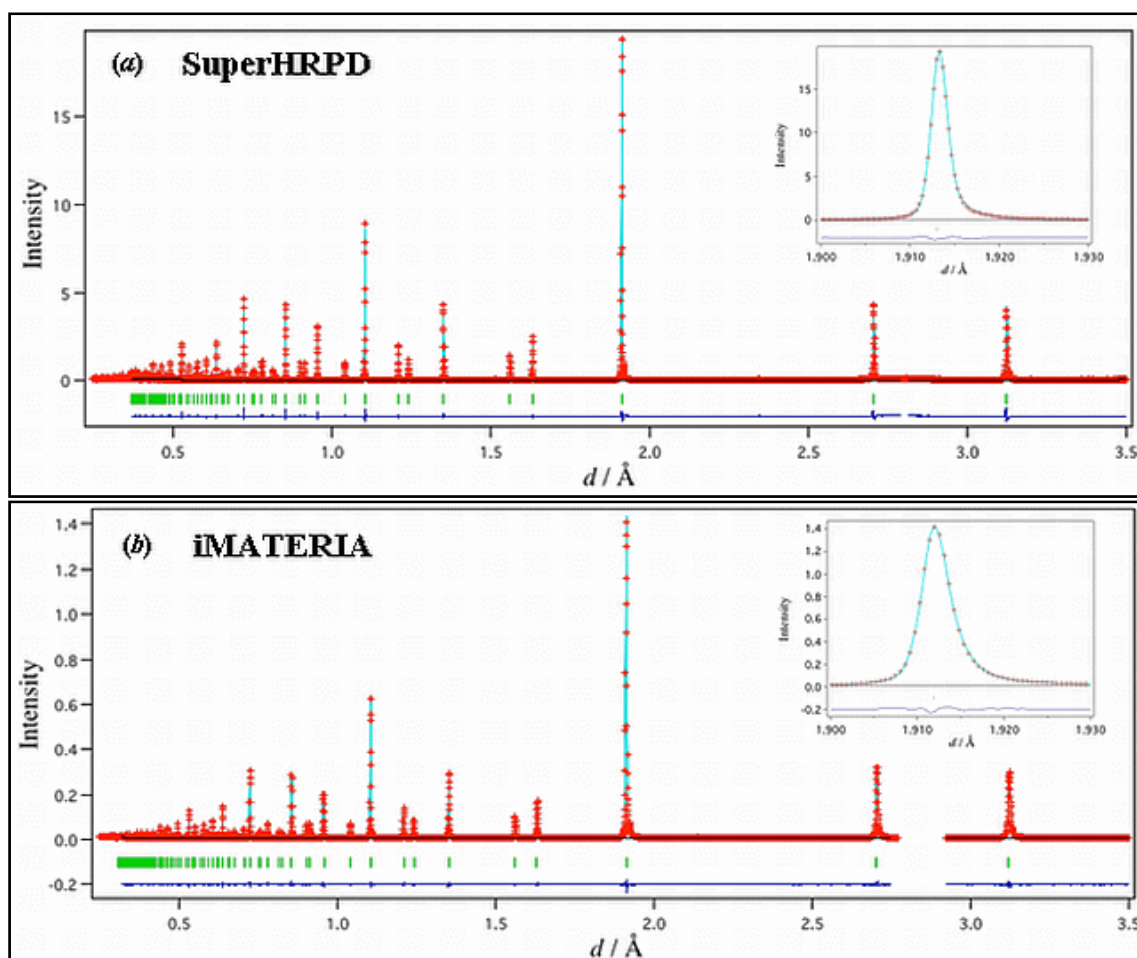


Figure 15: Rietveld refinement pattern of CeO_2 powder diffraction data taken from (a) SuperHRPD and (b) iMATERIA. The pattern shows observed (crosses), calculated (upper solid lines) and differences (lower solid lines) patterns. The positions of the Bragg peaks are given in the lower part as bars.

Table 4: Structural parameters for CeO_2 powder diffraction data taken from SuperHRPD and iMATERIA obtained through Rietveld analysis using Z-Rietveld.

	<i>SuperHRPD</i>	<i>iMATERIA</i>
$B_{(\text{Ce})}(\text{\AA}^2)$	0.244 (2)	0.247(2)
$B_{(\text{O})}(\text{\AA}^2)$	0.432 (2)	0.431(2)
R_{wp}	8.59%	4.72%
R_{e}	3.99%	2.22%
S^2	4.63	4.53
R_{p}	6.30%	4.22%
R_{B}	3.77%	1.04%
R_{F}	3.91%	2.33%

Space group: $Fm-3m$ $a = 5.411651\text{\AA}$

Occupancy: $\text{Ce} = 1$ and $\text{O} = 1$. Fractional coordinates for Ce : $x=y=z = 0$; for O :
 $x=y=z = 0.25$

2. Rietveld analysis of CeO₂ using Z-Rietveld.

The refinement result for CeO₂ powder diffraction data collected at SuperHRPD and iMATERIA are shown in Figure 15 and summary of the refinement are presented in Table 4. The comparison based on the diffraction patterns resulted by the two instruments shows that all Bragg peaks are well identified and are at the same positions. The inset in the two figures of magnified individual Bragg peaks (220) at position about 1.91 Å shows that the calculated profile is satisfactorily fits the observed profile.

CONCLUSION

SuperHRPD and iMATERIA are constructed to fulfill the demand of neutron powder diffractometer with suitable *d*-spacing resolution and range for experiment under special condition. SuperHRPD with best resolution in the world will enable the identification of individual intensities of Bragg reflection and to study more complicated structures. iMATERIA is a versatile neutron diffractometer with high throughput and is constructed to promote an industrial application for neutron beam. Z-Rietveld, has been developed as a software for the Rietveld analysis of powder diffraction data and proved to be reliable to analyze data taken from both diffractometers. The instrumental feature of SuperHRPD and iMATERIA supported by Z-Rietveld is effective in order to understand materials structure and to solve research problem in materials development.

ACKNOWLEDGMENT

TYSPP is grateful for all technical supports and discussions kindly given by researchers and institutes. Financial support by the Ministry of Education, Culture, Sport, Science and Technology (MEXT) – Japan is greatly acknowledged.

REFERENCES

- [1] T. Kamiyama et al., *Physica B* 213&214 (1995) 875-877
- [2] T. Ishigaki et al, *Nuclear Instruments and Methods in Physics Research A* 600 (2009) 189–191
- [3] J-PARC Homepage <http://j-parc.jp/MatLife/en/instrumentation/bl08/BL08.html>
- [4] KEK: Feature (NeutronSuperHRPD) <http://www.kek.jp/intra-e/feature/2010/NeutronSuperHRPD.html>
- [5] R. Oishi et al., *Nuclear Instruments and Methods in Physics Research A* 600 (2009) 94–96
- [6] User's guide for Z-Rietveld, High Energy Accelerator Research Organization
- [7] R.M. Brugger, *Mechanical and Time-of-flight Techniques*, in: P.A. Egelstaff (Ed.), *Thermal Neutron Scattering*, Academic Press, New York, 1965 (Chapter 2)
- [8] *The Rietveld Method*, edited by R.A. Young, International Union of Crystallography monographs on crystallography;5, Oxford University Press, 1996